

This discussion paper is/has been under review for the journal Drinking Water Engineering and Science (DWES). Please refer to the corresponding final paper in DWES if available.

# Development of a iron pipe corrosion simulation model for a water supply network

**M. Bernats<sup>1</sup>, S. W. Osterhus<sup>2</sup>, K. Dzelzitis<sup>3</sup>, and T. Juhna<sup>1</sup>**

<sup>1</sup>Department of Water Engineering and Technology, Riga Technical University, Latvia

<sup>2</sup>Department of Hydraulic and Environmental Engineering, Norwegian University of Science and Technology, Norway

<sup>3</sup>Department of Composite Materials and Structures, Riga Technical University, Latvia

Received: 17 February 2012 – Accepted: 19 March 2012 – Published: 2 April 2012

Correspondence to: T. Juhna (talis.juhna@rtu.lv)

Published by Copernicus Publications on behalf of the Delft University of Technology.

## Development of a iron pipe corrosion simulation model

M. Bernats et al.

Title Page

Abstract

Introduction

Conclusions

References

Tables

Figures



Back

Close

Full Screen / Esc

Printer-friendly Version

Interactive Discussion



## Abstract

Corrosion in water supply networks is unwanted process that causes pipe material loss and subsequent pipe failures. Nowadays pipe replacing strategy most often is based on pipe age, which is not always the most important factor in pipe burst rate. In this study a methodology for developing a mathematical model to predict the decrease of pipe thickness in a large cast iron networks is presented. The quality of water, the temperature and the water flow regime were the main factors taken into account in the corrosion model. The water quality and flow rate effect were determined by measuring corrosion rate of metals coupons over the period of one year at different flow regimes. The obtained constants were then introduced in a calibrated hydraulic model (Epanet) and the corrosion model was validated by measuring the decrease of wall thickness in the samples that were removed during the regular pipe replacing event. The validated model was run for 30 yr to simulate the water distribution system of Riga (Latvia). Corrosion rate in the first year was 8.0–9.5 times greater than in all the forthcoming years, an average decrease of pipe wall depth being 0.013/0.016 mm per year in long term. The optimal iron pipe exploitation period was concluded to be 30–35 yr (for pipe wall depth 5.50 mm and metal density  $7.5 \text{ m}^3 \text{ t}^{-1}$ ). The initial corrosion model and measurement error was 33 %. After the validation of the model the error was reduced to below 15 %.

## 1 Introduction

Iron pipe corrosion in water distribution networks is of a special concern for the drinking water industry, because of the large amount of unlined iron pipes that are in use nowadays. Corrosion consumes oxidants and disinfectants used for water treatment, create scales and loose deposits that increase the energy required for pumping, facilitates biofilm growth, and causes the discoloration of water (AWWA, 1996; Juhna, 2009). However, the main concern is leakage and breakage of pipes which creates significant

DWESD

5, 85–120, 2012

## Development of a iron pipe corrosion simulation model

M. Bernats et al.

Title Page

Abstract

Introduction

Conclusions

References

Tables

Figures



Back

Close

Full Screen / Esc

Printer-friendly Version

Interactive Discussion





## Development of a iron pipe corrosion simulation model

M. Bernats et al.

Title Page

Abstract

Introduction

Conclusions

References

Tables

Figures



Back

Close

Full Screen / Esc

Printer-friendly Version

Interactive Discussion

columns in which 12 steel coupons (st37) were placed parallel to the water flow. Before installation the coupons were cleaned, degreased and weighed. Measurements of the coupons were done every third month, by extracting 3 coupons from each column every time. Before the coupon extraction the feed line valve of the setup (not shown in the Fig. 1) was closed, shutting down the water feed to the setup without affecting the flow rate adjustments of the columns. The corrosion products/deposits were removed in ultrasonic bath followed by cleaning in concentrated HCl. Afterwards the coupons were dried (at 60 °C, for at least 4 h) and weighted.

The flow rate of column one (D1) was adjusted by valve A, and it was  $3.8 \pm 0.38 \text{ l min}^{-1}$  (denoted as “high flow rate”, with velocity  $0.35 \text{ m s}^{-1}$ ). The flow rate of column two (D2) was adjusted by valve B, and it was  $0.6 \pm 0.06 \text{ l min}^{-1}$  (denoted as “low flow rate”, with velocity  $0.05 \text{ m s}^{-1}$ ). The flow rate of column three (D3) was alternating between the high flow rate and stagnation (denoted as “alternating high flow rate and stagnation”). The alternation was determined by the timer which controls the solenoid valve. The timer was set to 11 h of stagnation followed by 13 h of flow, in total of 24 h period. The flow rate during the flowing period was adjusted by valve C, and it was  $3.8 \pm 0.38 \text{ l min}^{-1}$  (with velocity  $0.35 \text{ m s}^{-1}$ ). The flow rate of column four (D4) was alternating between high and low flow rate (denoted as “alternating high and low flow rates”). The alternation was determined by the same timer that controlled D3, which also controlled the solenoid valve in D4. The low flow rate had to be adjusted first with the solenoid valve closed. The low flow rate was then adjusted by valve D, and it was  $0.6 \pm 0.06 \text{ l min}^{-1}$  (with velocity  $0.05 \text{ m s}^{-1}$ ). After that the high flow rate was adjusted with the solenoid valve open. The high flow rate then was adjusted by valve E, and it was  $3.8 \pm 0.38 \text{ l min}^{-1}$  (with velocity  $0.35 \text{ m s}^{-1}$ ). The high flow rate was the sum of water flowing through valve D and E.

Water chemical parameters for which corrosion rates were established are shown in Table 1. For simplification purposes in the presented model two flow regimes (“high flow rate” and “low flow rate”) out of four regimes investigated were used.

## 2.2 Corrosion model

The corrosion model was built on founded corrosion expressions substituting it as multi species extension (MSX) quality sub model to a hydraulic model of Riga city, using a public domain software EPA Epanet 2.0. Applied hydraulic model was verified by means of electric conductivity (Juhna et al., 2009), i.e. detecting time of flow to pass between the nodes by measuring unique flow electric conduction. The hydraulic model of the water supply network of Riga was scaled to reflect the consumption of water by ~800 000 consumers assuming that the total water consumption was up to  $3.2 \times 10^5 \text{ m}^3 \text{ day}^{-1}$ , total pipe length (in model) ~200 km, pipe diameter ranging (in model) from DN100–1000 mm, mostly consisting from cast iron and steel pipes. Hydraulic and corrosion rates reporting the time steps for initial validation purposes was set for one hour after the validation increasing reporting time step to one day.

## 2.3 Collection and measurement of pipe examples

For validation of the corrosion model with established expressions, pipe samples of corresponding water supply network were collected. Pipe examples were collected from brakeage places of water mains of the water supply network. The samples were cut out in site, in form of continuous circular ring, about 20–30 cm in length. Afterwards in a workshop smaller segment was cut out (average size  $5 \times 10 \text{ cm}$ ). The segment from pipe to be analyzed was chosen such that the most pronounced corrosion formation on its inner wall was apparent. For obtaining the actual pipe wall depth, segments were scanned by ultrasonic measurement equipment “Hillgus” USPC 3010, Dr. Hillger Ultrasonic Techniques. The actual depth measurement was based on the assumption that due to the corrosion process delamination starts in the metal structure followed by gradual decrease of metal density. Thus ultrasonic signal is reflected in the deepest layer where pipe wall is unaffected and homogenous since further the structure of metal becomes delaminated and the signal is absorbed by micropores containing air. Initial or “zero” pipe wall depth value was taken from the Soviet time standards, when

DWESD

5, 85–120, 2012

## Development of a iron pipe corrosion simulation model

M. Bernats et al.

Title Page

Abstract

Introduction

Conclusions

References

Tables

Figures



Back

Close

Full Screen / Esc

Printer-friendly Version

Interactive Discussion



the water main was build (GOST 3262-75, 9567-75, 1050-88). In Fig. 2 an example of actual depth measurement of pipe wall by means of reflected ultrasonic sound is shown. For each example 7 depth measurements were taken using method shown in Fig. 2. The depth reading shown in Fig. 2 is  $430.0 - 425.6 = 4.4$  mm. The actual pipe wall depth measurement was taken between 2 or more reflection horizontals. For all pipe examples the average and minimal values of pipe wall depths was calculated. By subtraction of the initial depth, taken from manufacturing standards, and measurement, the average and the maximal decrease in pipe wall depth were obtained. Since the corrosion formulas in the model were calculated from data of average loss of mass, the average decrease in pipe wall depth was used for model validation. Maximal decrease of pipe wall depth was expressed as a linear function of average decrease. In further model simulations the maximal decrease was used since the time of the first breakage will occur from maximal corrosion rate.

Measurements were done using wet ultrasonic 5 MHz sensor which is used for composite materials. For depth readings raw ultrasonic reflective signal was used (without applying any filter) since applying filter for material surface with corrosion, containing micro air pours, signal will be not detectable. Initially the calibration of measurement device by changing sound expanding velocity in metal for polished steel pipe segment, with known depth measured by micrometer was done. It was found that measurements taken by the device and manually by the micrometer were similar at  $5700 \text{ m s}^{-1}$  speed of sound. By knowing the age of the pipe being in service and the metal density, depth measurements could be converted into corrosion rate (CR) using measurement conversion methodology. In Fig. 3 a map of Riga city water supply network with locations of pipe samples used in validation of corrosion model is shown.

## Development of a iron pipe corrosion simulation model

M. Bernats et al.

[Title Page](#)[Abstract](#)[Introduction](#)[Conclusions](#)[References](#)[Tables](#)[Figures](#)[Back](#)[Close](#)[Full Screen / Esc](#)[Printer-friendly Version](#)[Interactive Discussion](#)

## 2.4 Measurement converting methodology

Depth measurements were converted to actual corrosion rate (CR.meas) with following methodology:

$$\text{Loss of mass} = (h_{\text{initial}} - h_{\text{meas}}) \cdot 2\pi r \cdot 1 \cdot \rho = [t]$$

$$\text{Per square meter} = 1 / (2\pi r \cdot 1) = [\text{m}^2]$$

$$\text{Per day} = 365 \times \text{years} = [\text{day}]$$

$$\text{CR.meas} = \frac{((h_{\text{initial}} - h_{\text{meas}}) \cdot 2\pi r \cdot 1 \cdot \rho \cdot \frac{1}{(2\pi r \cdot 1)} \times 10^6)}{365 \times (\text{years} - 1)}$$

$$= \frac{(h_{\text{initial}} - h_{\text{meas}}) \cdot \rho \times 10^6}{365 \times (\text{years} - 1)} (\text{g m}^{-2} \text{ day}^{-1}) \quad (1)$$

where  $h_{\text{initial}}$  is initial depth of pipe wall from standards (m),  $h_{\text{meas}}$  – actual depth of pipe wall measurements (m),  $r$  – inner radius of pipe (m),  $1$  – longitudinal length of circumference for accuracy of dimensions (m),  $\rho$  – density of metal used in pipe manufacturing, years – number of years pipe being in service.

Multiplying equation by inverse circumference was based on fact that for each full square meter the lengths of both longitude and latitude should be 1, so on either side dimensions are square meters and circumference in denominator works as normalization of lost quantity of mass per square meter, reducing its value if circumference gives more than one or increasing its quantity if circumference gives less than one square meter. Data about pipe exploitation ages were collected from the archive of maintains enterprise of water supply network. The corresponding metal densities were described in manufacturing standards, with small variations in their value and generally being equal to  $7.5 \text{ t m}^{-3}$ .

Title Page

Abstract

Introduction

Conclusions

References

Tables

Figures



Back

Close

Full Screen / Esc

Printer-friendly Version

Interactive Discussion



## 2.5 Validation methodology

For validation of model corrosion rate (CR.mod) by measurements was done following methodology of Eqs. (2) and (3). It is mentioned that (CR.meas) of measurement is expressed from total lost mass, thus including first year corrosion constant ( $C$ ).

$$5 \quad \text{CR.mod} \times 365 (\text{years} - 1) + C \approx \text{Measurement (total lost mass)};$$

Since interest is about second stage corrosion rate (after first year constant),

$$\text{CR.mod} \approx \frac{\text{Measurement} - C}{365 (\text{years} - 1)}$$

After CR.model approximation on measurements,

$$\text{CR.mod} \cdot X1 \cong \frac{\text{Measurement}}{365 (\text{years} - 1)}$$

$$10 \quad [\text{CR.mod.v1} \times 365 (\text{years} - 1) \cdot X1 + C \cong \text{Measurement (for } v \leq 0.1 \text{ m s}^{-1})] \quad (2)$$

$$[\text{CR.mod.v2} \times 365 (\text{years} - 1) \cdot X2 + C \cong \text{Measurement (for } v > 0.1 \text{ m s}^{-1})] \quad (3)$$

where CR.mod.v1 is the corrosion rate for flow region 1 ( $v \leq 0.1 \text{ m s}^{-1}$ ), CR.mod.v2 – corrosion rate for flow region 2 ( $v > 0.1 \text{ m s}^{-1}$ ),  $X1$  – approximation function for the corrosion rate of flow region 1,  $X2$  – approximation function for corrosion rate of flow region 2,  $C$  – first year corrosion constant, since corrosion process development in first year is much faster until chemical equilibrium is achieved, Measurement – corresponding value of CR.meas.

Title Page

Abstract

Introduction

Conclusions

References

Tables

Figures



Back

Close

Full Screen / Esc

Printer-friendly Version

Interactive Discussion



### 3 Results

Exact model approximation on the corrosion process measurements is shown in Fig. 4. Two stages of corrosion process, in respect to time, were selected. In the first 360 days, the corrosion advances in considerably higher rate while the oxygen-limiting layer is formed. This step shows a semi-linear trend, with a gradual decrease of the slope. Since this stage has fixed time value till which it applies, it can be expressed as constant in long term simulations. In the model this constant was called first year constant ( $C_{\text{high}}$  for “high flow rate” and  $C_{\text{low}}$  for “low flow rate”). After the first 360 days the stage 2 starts, where corrosion happens at a lower rate and with constant value ( $CR_{\text{high}}$  for “high flow rate” and  $CR_{\text{low}}$  for “low flow rate”). The numerical values of Fig. 4 are shown in Table 2.

Based on approximated experimental data of rig tests, the corrosion rate expressions for stage 2 were established. The long term corrosion rate expressions were set as function only from mean hour flow velocity which changed the water temperature, all rest chemical parameters assuming constants.

Corrosion expressions established from corrosion rig tests are listed below, Eqs. (4) and (5), the dimensions are  $\text{g m}^{-2} \text{day}^{-1}$  (losed quantity, per square meter, per day).

$$CR.\text{mod}.v1 = \frac{0.27 \times 10^{10} \left( \frac{Cl^- + 2SO_4^{2-}}{\text{alk}} \right)^{0.4} \times e^{-(6000/(273+T))}}{(\text{pH} - 5) \cdot Ca^{0.2}} \quad (\text{for } v \leq 0.1 \text{ m s}^{-1}) \quad (4)$$

$$CR.\text{mod}.v2 = \frac{0.65 \times 10^{10} \left( \frac{Cl^- + 2SO_4^{2-}}{\text{alk}} \right)^{0.2} \times e^{-(6000/(273+T))}}{\text{pH} \cdot Ca^{0.1}} \quad (\text{for } v > 0.1 \text{ m s}^{-1}) \quad (5)$$

where pH is potential of hydrogen ion concentration, Ca – calcium ( $\text{mg l}^{-1}$ ),  $T$  – water temperature ( $^{\circ}\text{C}$ ), Alk – alkalinity ( $\text{mmol l}^{-1}$ ),  $Cl^-$  – total chlorine ( $\text{mmol l}^{-1}$ ),  $SO_4^{2-}$  – sulphate ( $\text{mmol l}^{-1}$ ).

Title Page

Abstract

Introduction

Conclusions

References

Tables

Figures

⏪

⏩

◀

▶

Back

Close

Full Screen / Esc

Printer-friendly Version

Interactive Discussion



## Development of a iron pipe corrosion simulation model

M. Bernats et al.

Title Page

Abstract

Introduction

Conclusions

References

Tables

Figures

⏪

⏩

◀

▶

Back

Close

Full Screen / Esc

Printer-friendly Version

Interactive Discussion



The difference function graphic is shown in Fig. 5 and the corresponding numerical values are shown in Table 3. For each flow region a different function was approximated. It is important to note that the relation between corrosion rates CR.mod.v1 ( $v \leq 0.1 \text{ m s}^{-1}$ ) and CR.mod.v2 ( $v > 0.1 \text{ m s}^{-1}$ ) is not constant, i.e. for value  $\text{pH} \leq 6.45$ , CR.mod.v1  $>$  CR.mod.v2, but for  $\text{pH} > 6.45$ , CR.mod.v1  $<$  CR.mod.v2. Generally pH value of  $\leq 6.45$  characterizes surface water, but pH value of  $> 6.45$  underground waters. The interrelation between CR.mod values as function of pH is shown in Fig. 6.

In Fig. 7 the error range of initial and validated corrosion model is shown. The corresponding numerical values and additional information about pipe samples are shown in Table 4. The maximal corrosion rate as function from average corrosion rate is shown in Fig. 8. After model validation with average corrosion rates the maximum corrosion rate values were used for long term simulations.

There is a linear, positive relationship, between the corrosion rate (established from measurements) and flow velocities (determined from validated hydraulic model), e.g. CR (rate,  $\text{g m}^{-2} \text{ day}^{-1}$ ) = 0.24 (velocity,  $\text{m s}^{-1}$ ) + 0.31 (Fig. 9).

Corrosion expressions after validation are as follows:

$$[\text{CR.mod.v1} \times 365 (\text{years} - 1)] \cdot (1.7\bar{v} + 1.2) + C \quad (\text{for } v \leq 0.1 \text{ m s}^{-1}) \quad (6)$$

$$[\text{CR.mod.v2} \times 365 (\text{years} - 1)] \cdot (0.82\bar{v}^{-0.22}) + C \quad (\text{for } v > 0.1 \text{ m s}^{-1}) \quad (7)$$

where CR.mod.v1 and CR.mod.v2 is initial corrosion expressions, Eqs. (4) and (5) ( $\text{g m}^{-2} \text{ day}^{-1}$ ), years – number of years pipe being in service,  $\bar{v}$  – average flow velocity ( $\text{m s}^{-1}$ ),  $C$  – first year constants, for  $v \leq 0.1 \text{ m s}^{-1}$   $C = 635 \text{ g m}^{-2}$ , for  $v > 0.1 \text{ m s}^{-1}$   $C = 785 \text{ g m}^{-2}$ .

## 4 Discussion

The values of validated model are the values of the initial model multiplied by difference functions, i.e. Eqs. (6) and (7), obtained from Fig. 5. The corresponding initial

and validated model error ranges are shown in Fig. 7. Initially model values versus measurement values fit relatively well, mostly because of the fact that the theoretical formulas were calculated from the same water supply network from which the pipe samples were taken, thus water chemical content remained constant. After the validation of the model the error was reduced to 15%. The difference functions were set so that the model after validation gives only positive error. Thereby the model is more reliable by giving a corrosion brakeage warning at maximum 15% earlier, which involves noticeably less emergency costs than in a case of delayed brakeage warning. The difference function  $X1$  and  $X2$  for the validated model were calculated as the difference ratio between measured value and the expected value obtained from the model. Then difference ratio was plotted versus daily average flow velocity of hydraulic model and for each flow region (1. region  $v \leq 0.1 \text{ m s}^{-1}$ , 2. region  $v > 0.1 \text{ m s}^{-1}$ ) the difference function was calculated. The greatest difference between the model and the measurements is for the 1st region ( $v \leq 0.1 \text{ m s}^{-1}$ ), therefore a linear difference function  $y = 1.7x + 1.2$  was found. In the case of flow velocity  $v = 0 \text{ m s}^{-1}$  the initial model value was increased by 20%. A difference function for 2nd region ( $v > 0.1 \text{ m s}^{-1}$ ) was found  $y = 0.82x^{-0.22}$ , which gradually joins to only point of 2nd region measurement. For 2nd region was chosen power function, because there is only one measurement point and it match good with model, so difference function should decrease more faster than linear function.

In Eqs. (4) and (5) is shown established corrosion rate expressions for both flow regions, Eq. (4) for  $v \leq 0.1 \text{ (m s}^{-1}\text{)}$ , and Eq. (5)  $v > 0.1 \text{ (m s}^{-1}\text{)}$ . This system of two equations in respect to flow velocity is explained by observing different oxygen transferring quantity between water flow and corrosion layer. This different oxygen transferring quantity does not have constant relationship between both corrosion Eqs. (4) and (5) in respect to corrosion rate. This relationship was determined by pH value, which is a constant parameter in both Eqs. (4) and (5). The interrelation of corrosion rates Eqs. (4) and (5) as function from pH is shown in Fig. 6. The border value at which the flow region 1 ( $v \leq 0.1 \text{ m s}^{-1}$ ) should be greater in corrosion rate than flow

**Development of a  
iron pipe corrosion  
simulation model**

M. Bernats et al.

[Title Page](#)[Abstract](#)[Introduction](#)[Conclusions](#)[References](#)[Tables](#)[Figures](#)[Back](#)[Close](#)[Full Screen / Esc](#)[Printer-friendly Version](#)[Interactive Discussion](#)

region 2 ( $v > 0.1 \text{ m s}^{-1}$ ) is from  $\text{pH} \leq 6.45$ . Usually the water with  $\text{pH} \leq 6.45$  is surface source water, while water with  $\text{pH} > 6.45$  comes from groundwater source, so in general groundwater will correspond to relationship  $\text{CR.mod.v1} < \text{CR.mod.v2}$ , but the surface water will correspond to relationship  $\text{CR.mod.v1} > \text{CR.mod.v2}$ . The maximal corrosion rate was expressed as linear function from average corrosion rate, based on measurement data of pipe samples (Fig. 8).

The correlation between the corrosion rate ( $\text{g m}^{-2} \text{ day}^{-1}$ ) and the flow velocity ( $\text{m s}^{-1}$ ) is of special interest, since it establishes a direction of the corrosion process as function from flow velocity (Fig. 9). However this correlation is obtained only from the pipe samples of the righth bank of network, which in accordance of the hydraulic model data, generally is supplied by water WTP-B. Therefore the correlation in Fig. 9 is valid only for groundwater source supplied networks ( $\text{pH} > 6.45$ ). Theoretically the correlation between the corrosion rate and the flow velocity for network part supplied by WTP-D (surface water source,  $\text{pH} \leq 6.45$ ) should be inversely negative to the correlation of Fig. 9.

Further results of corrosion model simulations, shown in appendix, are discussed. The corrosion rates of network links in the first year ( $A1, \text{g m}^{-2} \text{ yr}^{-1}$ ) and all forthcoming years after the first year ( $A2, \text{g m}^{-2} \text{ day}^{-1}$ ) are shown in the Appendix A. The all following data calculations were based on these values. The total corroded mass ( $\text{g m}^{-2}$ ) after the first year ( $B1$ ), after the tenth year ( $B2$ ), and after the thirtieth year ( $B3$ ) is represented in Appendix B. The corrosion depths of pipe walls (mm), assuming that steel density used in pipes is  $\rho_{\text{steel}} = 7.5 \text{ t m}^{-3}$ , after first year ( $C1$ ), after tenth year ( $C2$ ), and after thirtieth year ( $C3$ ) are shown in Appendix C.

The most graphic effect of corrosion in water supply network can be seen in Appendix C where after first year there was a jump in pipe wall decrease from which biggest values can be seen even in 5 yr legend, this is due the corrosion constant. Afterwards the corrosion rate continued to increase with a constant rate. The average step of corrosion mass was about  $100\text{--}120 \text{ g m}^{-2} \text{ yr}^{-1}$ , which using Eq. (1) from the measurement converting methodology and assuming that the metal density is

## Development of a iron pipe corrosion simulation model

M. Bernats et al.

Title Page

Abstract

Introduction

Conclusions

References

Tables

Figures



Back

Close

Full Screen / Esc

Printer-friendly Version

Interactive Discussion



equal to  $7.5 \text{ t m}^{-3}$ , gives the corresponding average decrease of actual pipe depth by 0.013/0.016 mm per year (0.1 mm per 6.2/7.5 yr). As mentioned before in the validated model simulations maximal corrosion rate was used since the pipe will break in point of maximal corrosion and in time of maximal rate. According to Fig. 8 maximal corrosion rate is the average rate multiplied by 1.80.

From model simulations it was calculated that corrosion safe exploitation period, for standard steel pipes, with clear metal thickness of 5.50 mm, which corresponds to commercial diameter range from DN100–DN300 mm, is in range of 30–35 yr. For further corrosion reducing studies, attention should be directed to methods which reduce the value of relationship  $\text{CR.max/CR.mean}$  in water treatment process, since by reducing this ratio, the service time of water mains will proportionally increase. In the current study the validation of the corrosion model was done only for one bank of city water supply network (marked with arrows) which is supplied by groundwater source water from WTP-B. Consequently for the corrosion model validation in water supply network or its part supplied by surface water source additional validation should be done in the future. It is important to note that the largest disadvantage of the field trials for considered as a statically stable studies is the small number of validation measurements ( $n \ll 30$ ). It is still believed that behavior of this corrosion model is correct, thereby with increase of sample number the accurateness of this model will increase.

## 5 Conclusions

From this study the following conclusions can be drawn:

1. There is a significant positive correlation, for underground source water, between the corrosion rate on pipe wall inner surface and the flow velocity.
2. The surface source water causes approximately two times faster corrosion of a water supply network by means of the average corrosion rate, with the average corrosion rate  $0.48 \text{ g m}^{-2} \text{ day}^{-1}$ , than underground source water, with the average

## Development of a iron pipe corrosion simulation model

M. Bernats et al.

Title Page

Abstract

Introduction

Conclusions

References

Tables

Figures



Back

Close

Full Screen / Esc

Printer-friendly Version

Interactive Discussion



corrosion rate  $0.23 \text{ g m}^{-2} \text{ day}^{-1}$ , after the oxygen-limiting layer is formed in the first year.

3. Optimal time of exploitation, for commercial diameter range from diameter 100 to 300 mm, for cast iron and steel pipes is in range of 30–35 yr, if the initial metal layer thickness of the pipe wall is 5.50 mm.
4. The validated corrosion model, Eqs. (6) and (7) with error less than 15 % can be used for another water supply network, supplied by underground water source with similar water chemical properties to Riga city WTP-B. Otherwise the use of corrosion Eqs. (4) and (5) must be validated with approximation on field measurements.

*Acknowledgements.* This work has been undertaken as a part of the research project “Technology enabled universal access to safe water – TECHNEAU” (Nr. 018320) which is supported by the European Union within the 6th Framework Programme. There hereby follows a disclaimer stating that the authors are solely responsible for the work. It does not represent the opinion of the Community and the Community is not responsible for any use that might be made of data appearing herein. Senior researcher (RTU) Janis Rubulis is gratefully acknowledged for valuable advices and guidance along the work. Kaspars Kalnins is gratefully acknowledged for significant measurement advices.

## References

- AWWA Research foundation: Internal corrosion of water distribution systems, Cooperative research report, 2nd Edn., 1996.
- AWWA Research foundation: Corrosion in a distribution system: steady water and its composition, Water Res., 44, 1872–1883, 2010.
- Juhna, T. and Osterhus, S. W.: Modelling of regrowth in water distribution network, TECHNEAU and SECUREAU Conference, 12 December 2009.

## Development of a iron pipe corrosion simulation model

M. Bernats et al.

Title Page

Abstract

Introduction

Conclusions

References

Tables

Figures



Back

Close

Full Screen / Esc

Printer-friendly Version

Interactive Discussion



## Development of a iron pipe corrosion simulation model

M. Bernats et al.

Title Page

Abstract

Introduction

Conclusions

References

Tables

Figures



Back

Close

Full Screen / Esc

Printer-friendly Version

Interactive Discussion



- Juhna, T., Gruskevica, K., Tihomirova, K., and Osterhus, S. W.: Influence of water velocity and NOM composition on corrosion of cast iron and copper, METEAU Conference, 29–31 October 2008.
- Laycock, N., Laycock, P., Scarf, P., and Krouse, D.: Applications of statistical analysis techniques in corrosion experimentation, testing, inspection and monitoring, Shreir's Corrosion, chapter 2.36, 1547–1580, 2010.
- McIntyre, P. J. and Mercer, A. D.: Corrosion testing and determination of corrosion rates, Shreir's Corrosion, chapter 2.34, 1443–1526, 2010.
- Naser, G. and Karney, B. W.: A 2-D transient multi component simulation model: application to pipe wall corrosion, Journal of Hydro-Environment Research, 1, 56–69, 2007.
- Sarin, P., Snoeyink, V. L., Bebee, J., Kriven, W. M., and Clement, J. A.: Physico-chemical characteristics of corrosion scales in old iron pipes, Water Res., 35, 2961–2969, 2001.
- Vargas, I. T., Pasten, P. A., and Pizarro, G. E.: Empirical model for dissolved oxygen depletion during corrosion of drinking water copper pipes, Corros. Sci., 52, 2250–2257, doi:10.1016/j.corsci.2010.03.009, 2010.

## Development of a iron pipe corrosion simulation model

M. Bernats et al.

Title Page

Abstract

Introduction

Conclusions

References

Tables

Figures

⏪

⏩

◀

▶

Back

Close

Full Screen / Esc

Printer-friendly Version

Interactive Discussion



**Table 1.** Average values of water chemical parameters in WTP B and D.

Water quality parameter	B		D	
	Average	SD ±	Average	SD ±
pH	7.57	0.15	6.91	0.26
Ca, mg l <sup>-1</sup>	63.36	5.75	52.13	6.28
Alkalinity, mg l <sup>-1</sup>	184.00	10.16	130.13	29.77
Temperature, °C	10.62	2.59	8.65	8.03
SO <sub>4</sub> <sup>2-</sup> , mg l <sup>-1</sup>	62.26	3.85	80.74	4.94
Cl <sup>-</sup> , mg l <sup>-1</sup>	119.00		8.56	
Mg, mg l <sup>-1</sup>	17.74	1.14	12.48	1.63
Mn, mg l <sup>-1</sup>	0.07	0.03	0.01	0.01
Si, mg l <sup>-1</sup>	2.99	0.79	2.15	1.13
Conductivity, μS cm <sup>-2</sup>	754.06	105.63	358.45	152.56
Turbidity, NTU	0.54	0.09	0.20	0.11
Fe-tot, mg l <sup>-1</sup>	0.21	0.08	0.05	0.00
Redox, mV vs. AgCl	257.82	30.80	260.61	127.02
Dissolved oxygen, mg l <sup>-1</sup>	7.91	1.34	22.96	11.45
DOC, mg Cl <sup>-1</sup>	5.03	1.02	5.84	1.13
BDOC, mg Cl <sup>-1</sup>	0.47	0.35	0.58	0.26
P-tot, mg l <sup>-1</sup>	0.01	0.01	0.02	0.04
N-tot, mg l <sup>-1</sup>	0.49	0.21	1.11	0.77
Cl <sub>2</sub> -tot, mg l <sup>-1</sup>	0.13	0.07	0.02	0.01

## Development of a iron pipe corrosion simulation model

M. Bernats et al.

Title Page

Abstract

Introduction

Conclusions

References

Tables

Figures

⏪

⏩

◀

▶

Back

Close

Full Screen / Esc

Printer-friendly Version

Interactive Discussion



**Table 2.** Numerical values of approximation of corrosion process ( $\text{g m}^{-2} \text{day}^{-1}$ ) dynamics.

Days	High flow rate ( $v > 0.1 \text{ m s}^{-1}$ )	Low flow rate ( $v \leq 0.1 \text{ m s}^{-1}$ )	H/O flow rate ( $v = 0.2/0 \text{ m s}^{-1}$ )	H/L flow rate ( $v = 0.2/0.03 \text{ m s}^{-1}$ )
88	3.38	2.44	2.47	3.15
174	2.49	1.83	1.73	2.15
249	2.02	1.51	1.47	1.83
335	1.68	1.18	1.19	1.47
Short term (average)	2.39	1.74	1.72	2.15
Long term	0.30	0.19	0.21	0.23

**Development of a  
iron pipe corrosion  
simulation model**

M. Bernats et al.

Title Page

Abstract

Introduction

Conclusions

References

Tables

Figures



Back

Close

Full Screen / Esc

Printer-friendly Version

Interactive Discussion



**Table 3.** Difference function values.

Sample	Diameter (mm)	CR.mod (g m <sup>-2</sup> day <sup>-1</sup> )	CR.meas (g m <sup>2</sup> day <sup>-1</sup> )	Meas./mod. (-)	V_day_mean (m s <sup>-1</sup> )
1.	150	0.270	0.329	1.22	0.02
2.	500	0.281	0.301	1.07	0.02
3.	300	0.395	0.400	1.01	0.38
4.	300	0.242	0.322	1.33	0.08

Sample	Func.X1 (-)	Func.X2 (-)	CR.mod · X1 (g m <sup>-2</sup> day <sup>-1</sup> )	CR.mod · X2 (g m <sup>-2</sup> day <sup>-1</sup> )	Valid error (-)
1.	1.23	–	0.333	–	1.27 %
2.	1.23	–	0.347	–	15.20 %
3.	–	1.01	–	0.401	0.18 %
4.	1.34	–	0.323	–	0.41 %

Development of a  
iron pipe corrosion  
simulation model

M. Bernats et al.

Title Page

Abstract

Introduction

Conclusions

References

Tables

Figures



Back

Close

Full Screen / Esc

Printer-friendly Version

Interactive Discussion



**Table 4.** Pipe sample parameters and error range values.

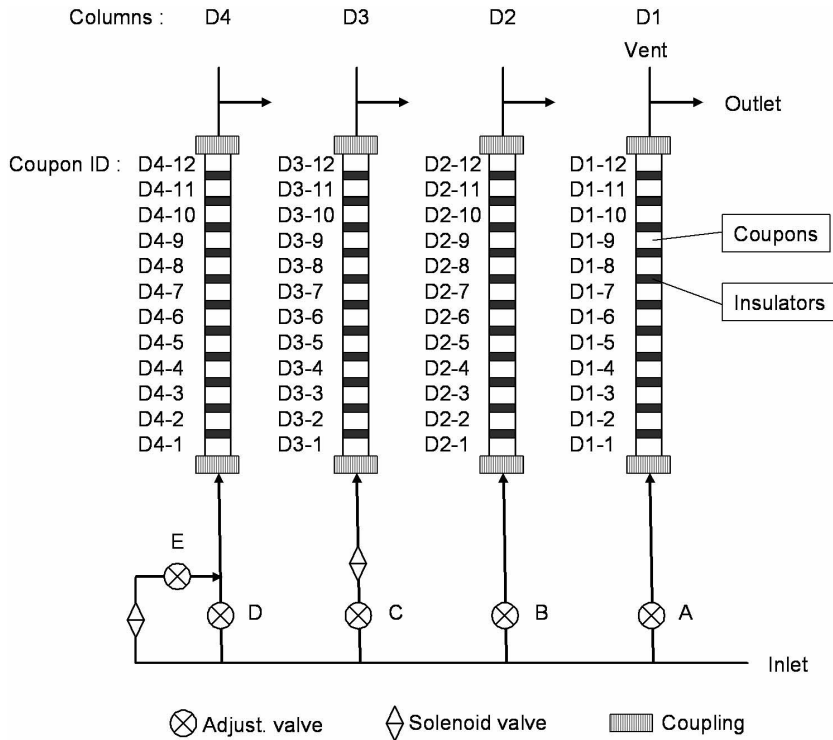
Sample	Diameter (mm)	Actual depth		Initial depth (mm)	$\Delta h$ average (mm)
		average (mm)	minimal (mm)		
1.	150	4.96	4.60	5.50	0.54
2.	500	6.95	6.70	7.50	0.55
3.	300	5.09	4.75	5.50	0.41
4.	300	12.00	11.65	12.70	0.70

Sample	Age (years)	V_day_mean ( $\text{m s}^{-1}$ )	CR.meas ( $\text{g m}^{-2} \text{day}^{-1}$ )	CR.mod-valid ( $\text{g m}^{-2} \text{day}^{-1}$ )	Valid error (–)
1.	27	0.02	0.329	0.333	1.27 %
2.	30	0.02	0.301	0.347	15.20 %
3.	17	0.38	0.400	0.401	0.18 %
4.	38	0.08	0.322	0.323	0.41 %

## Development of a iron pipe corrosion simulation model

M. Bernats et al.



**Fig. 1.** Schematic sketch of test rig experiments for various flow velocities (in both WTP, B and D).

Title Page

Abstract

Introduction

Conclusions

References

Tables

Figures

⏪

⏩

◀

▶

Back

Close

Full Screen / Esc

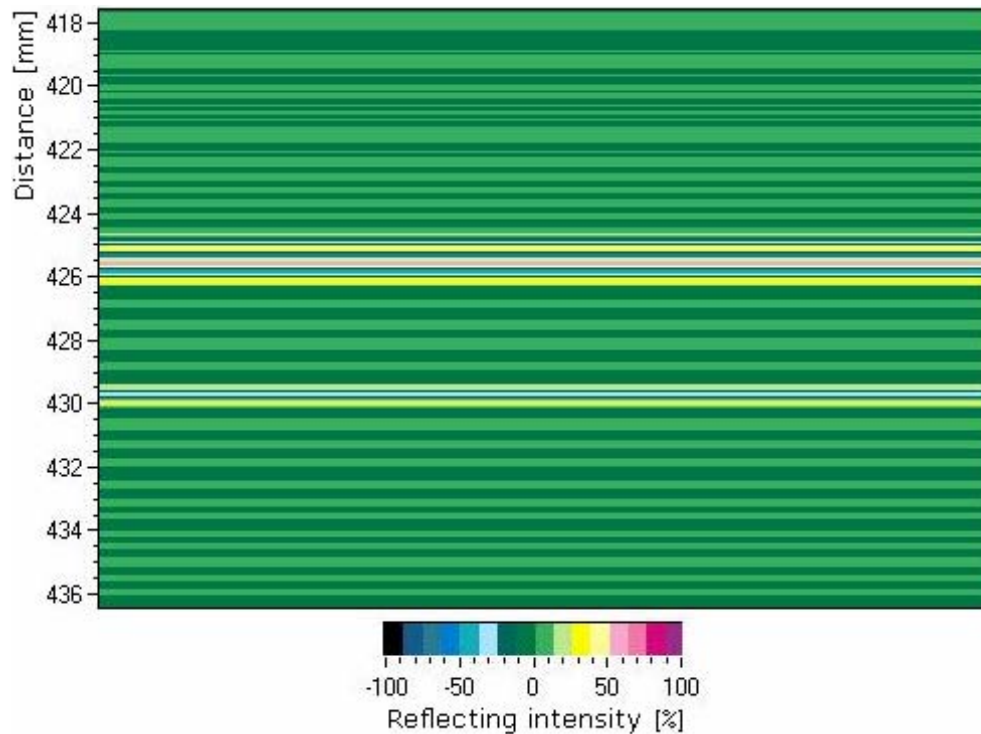
Printer-friendly Version

Interactive Discussion



**Development of a  
iron pipe corrosion  
simulation model**

M. Bernats et al.

**Fig. 2.** Measurement of pipe wall depth.[Title Page](#)[Abstract](#)[Introduction](#)[Conclusions](#)[References](#)[Tables](#)[Figures](#)[⏪](#)[⏩](#)[◀](#)[▶](#)[Back](#)[Close](#)[Full Screen / Esc](#)[Printer-friendly Version](#)[Interactive Discussion](#)

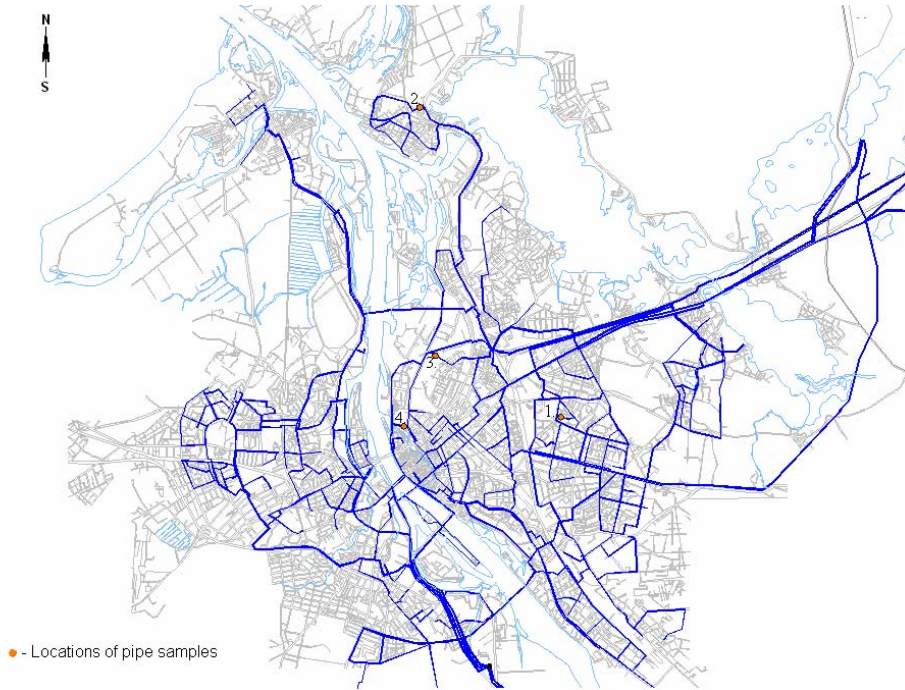


**Fig. 3.** Locations of pipe samples used of model validation.

**Development of a  
iron pipe corrosion  
simulation model**

M. Bernats et al.

Title Page

Abstract

Introduction

Conclusions

References

Tables

Figures



Back

Close

Full Screen / Esc

Printer-friendly Version

Interactive Discussion





Development of a  
iron pipe corrosion  
simulation model

M. Bernats et al.

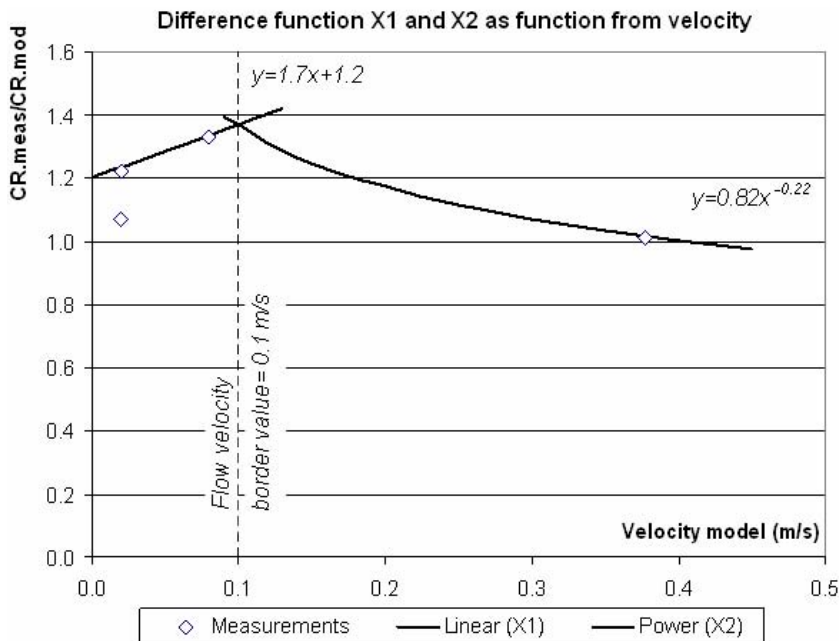


Fig. 5. Difference functions X1 and X2 of validated model.

Title Page

Abstract

Introduction

Conclusions

References

Tables

Figures

⏪

⏩

◀

▶

Back

Close

Full Screen / Esc

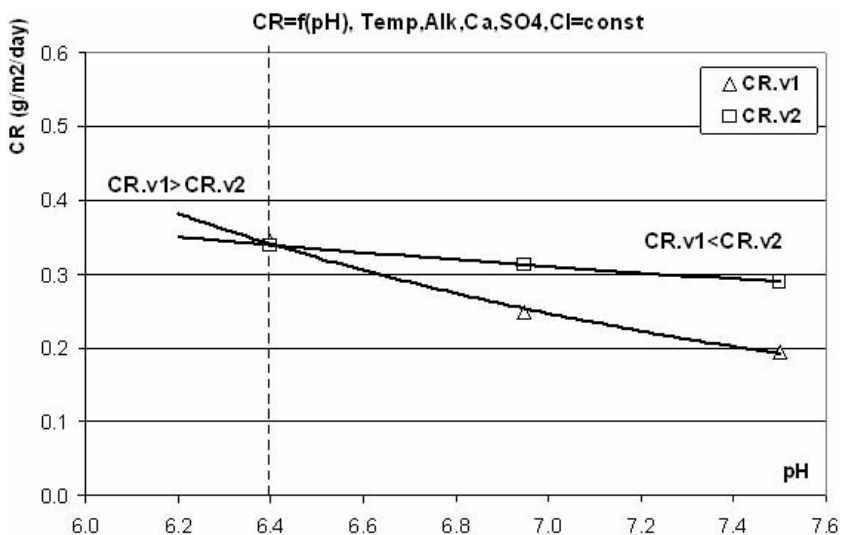
Printer-friendly Version

Interactive Discussion



**Development of a  
iron pipe corrosion  
simulation model**

M. Bernats et al.

**Fig. 6.** Interrelation between CR.mod.v1 and CR.mod.v2 as function from pH.[Title Page](#)[Abstract](#)[Introduction](#)[Conclusions](#)[References](#)[Tables](#)[Figures](#)[⏪](#)[⏩](#)[⏴](#)[⏵](#)[Back](#)[Close](#)[Full Screen / Esc](#)[Printer-friendly Version](#)[Interactive Discussion](#)

Development of a  
iron pipe corrosion  
simulation model

M. Bernats et al.

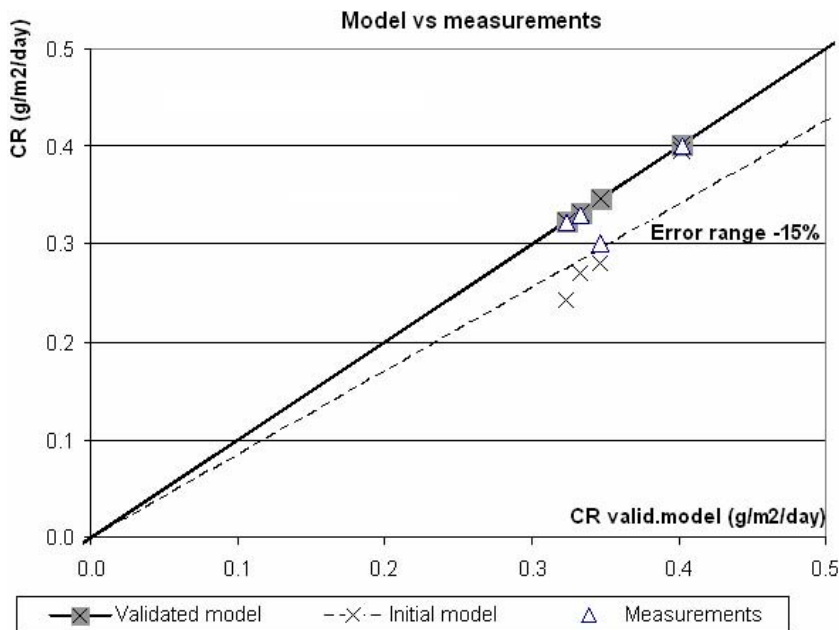


Fig. 7. Error range of initial and validated corrosion model.

Title Page

Abstract

Introduction

Conclusions

References

Tables

Figures

⏪

⏩

◀

▶

Back

Close

Full Screen / Esc

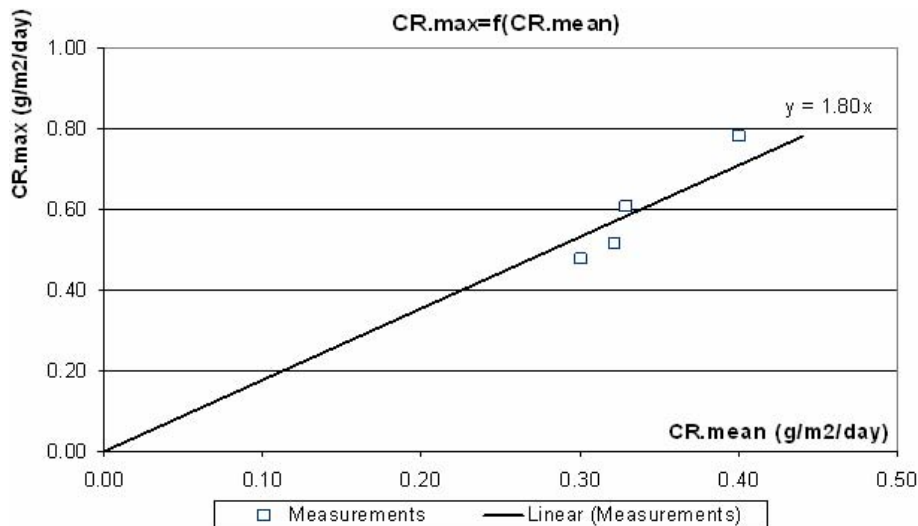
Printer-friendly Version

Interactive Discussion



**Development of a  
iron pipe corrosion  
simulation model**

M. Bernats et al.

[Title Page](#)[Abstract](#)[Introduction](#)[Conclusions](#)[References](#)[Tables](#)[Figures](#)[⏪](#)[⏩](#)[⏴](#)[⏵](#)[Back](#)[Close](#)[Full Screen / Esc](#)[Printer-friendly Version](#)[Interactive Discussion](#)**Fig. 8.** Maximal corrosion rate as function from average corrosion.

Development of a  
iron pipe corrosion  
simulation model

M. Bernats et al.

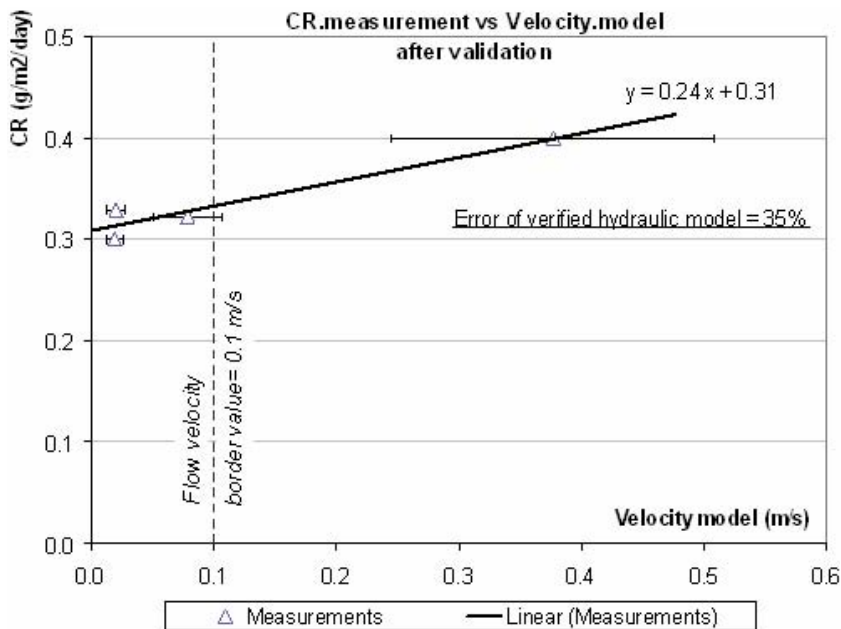


Fig. 9. Correlation between corrosion rates of measurements and flow velocities of hydraulic model.

Title Page

Abstract

Introduction

Conclusions

References

Tables

Figures

⏪

⏩

◀

▶

Back

Close

Full Screen / Esc

Printer-friendly Version

Interactive Discussion



Development of a  
iron pipe corrosion  
simulation model

M. Bernats et al.

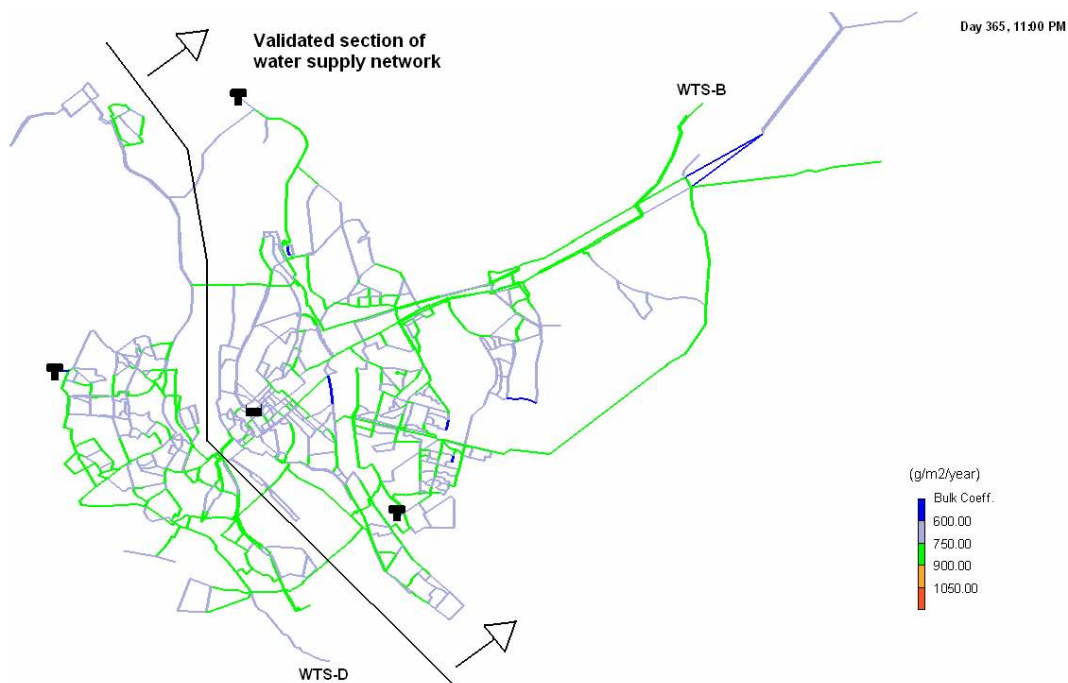


Fig. A1. Corrosion rate constants (C) of 1st year ( $\text{g m}^{-2} \text{yr}^{-1}$ ).

Title Page

Abstract

Introduction

Conclusions

References

Tables

Figures

⏪

⏩

⏴

⏵

Back

Close

Full Screen / Esc

Printer-friendly Version

Interactive Discussion



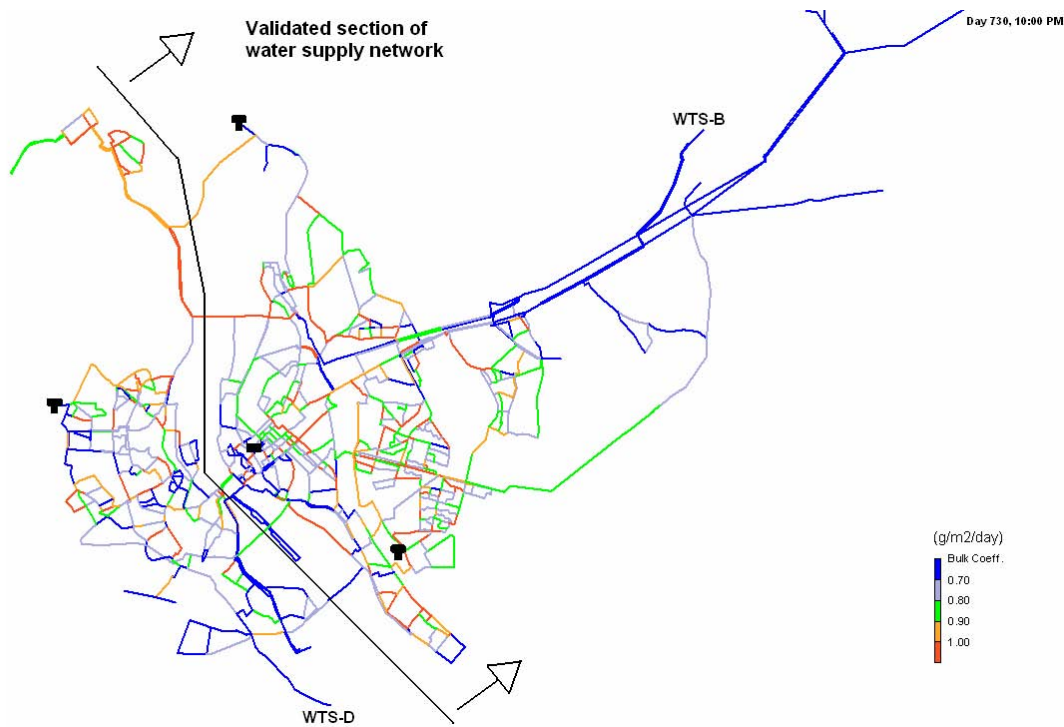


**Fig. A2.** Corrosion rate (CR) in all forthcoming years, after first 1st year ( $\text{g m}^{-2} \text{day}^{-1}$ ).

**Development of a  
iron pipe corrosion  
simulation model**

M. Bernats et al.

Title Page

Abstract

Introduction

Conclusions

References

Tables

Figures

⏪

⏩

⏴

⏵

Back

Close

Full Screen / Esc

Printer-friendly Version

Interactive Discussion



Development of a  
iron pipe corrosion  
simulation model

M. Bernats et al.

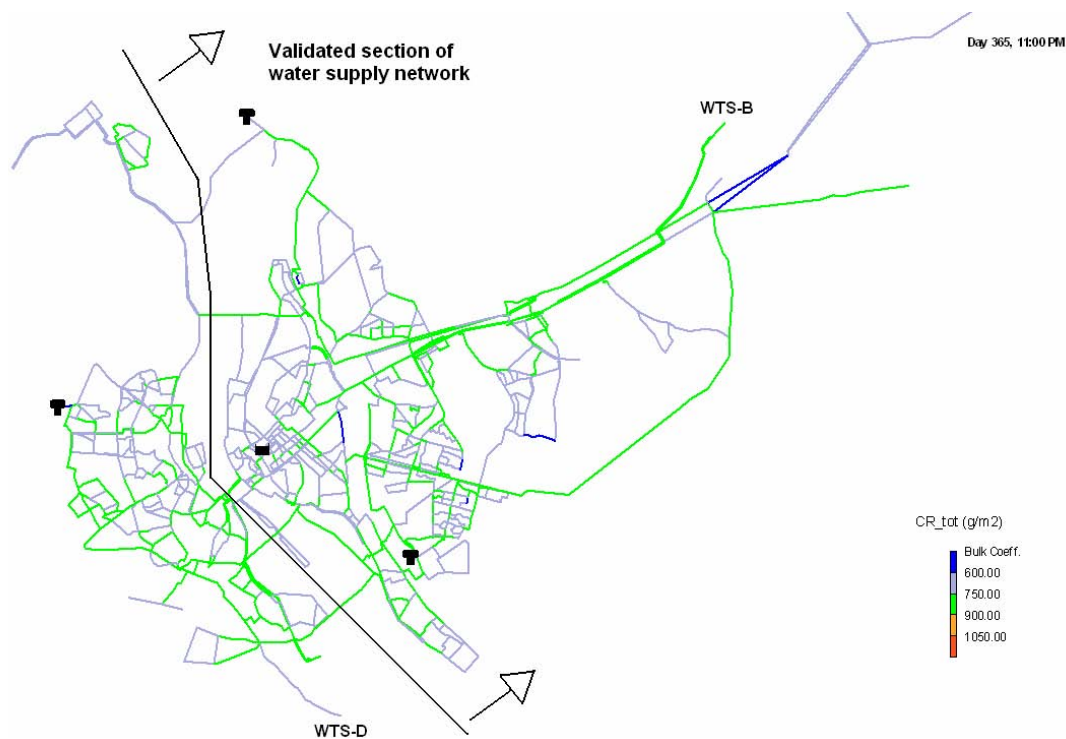


Fig. B1. Total corroded mass after 1st year ( $\text{g m}^{-2}$ ).

Title Page

Abstract

Introduction

Conclusions

References

Tables

Figures

⏪

⏩

◀

▶

Back

Close

Full Screen / Esc

Printer-friendly Version

Interactive Discussion



Development of a  
iron pipe corrosion  
simulation model

M. Bernats et al.

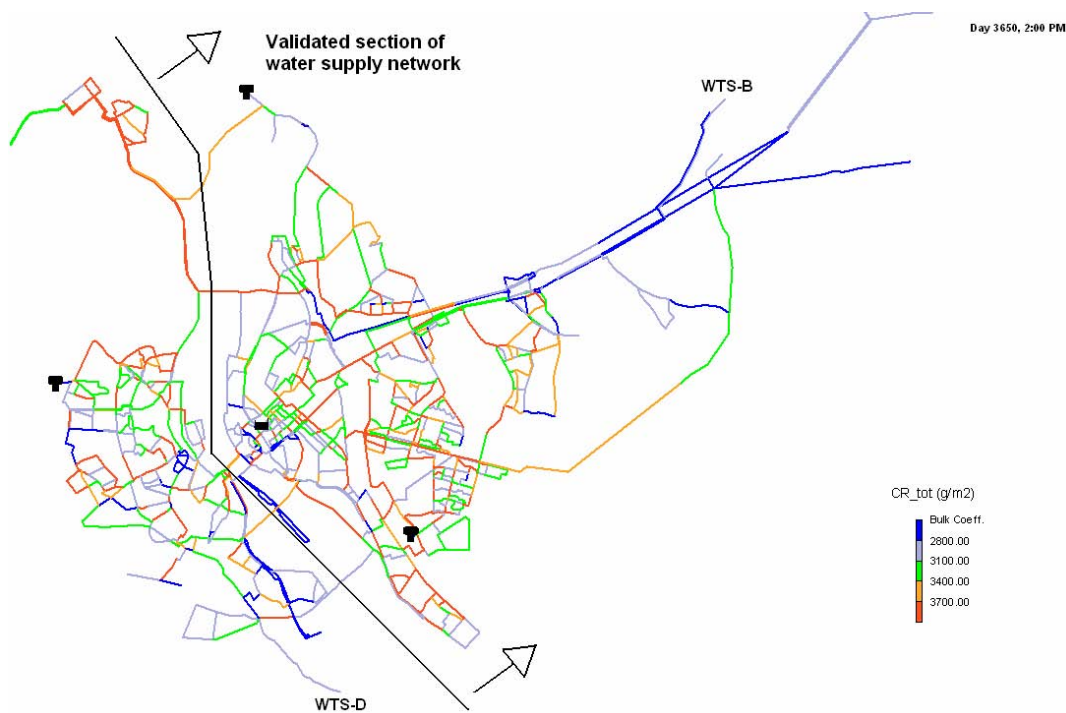


Fig. B2. Total corroded mass after 10th year ( $\text{g m}^{-2}$ ).

Discussion Paper | Discussion Paper | Discussion Paper | Discussion Paper | Discussion Paper

Title Page

Abstract

Introduction

Conclusions

References

Tables

Figures

⏪

⏩

⏴

⏵

Back

Close

Full Screen / Esc

Printer-friendly Version

Interactive Discussion



## Development of a iron pipe corrosion simulation model

M. Bernats et al.

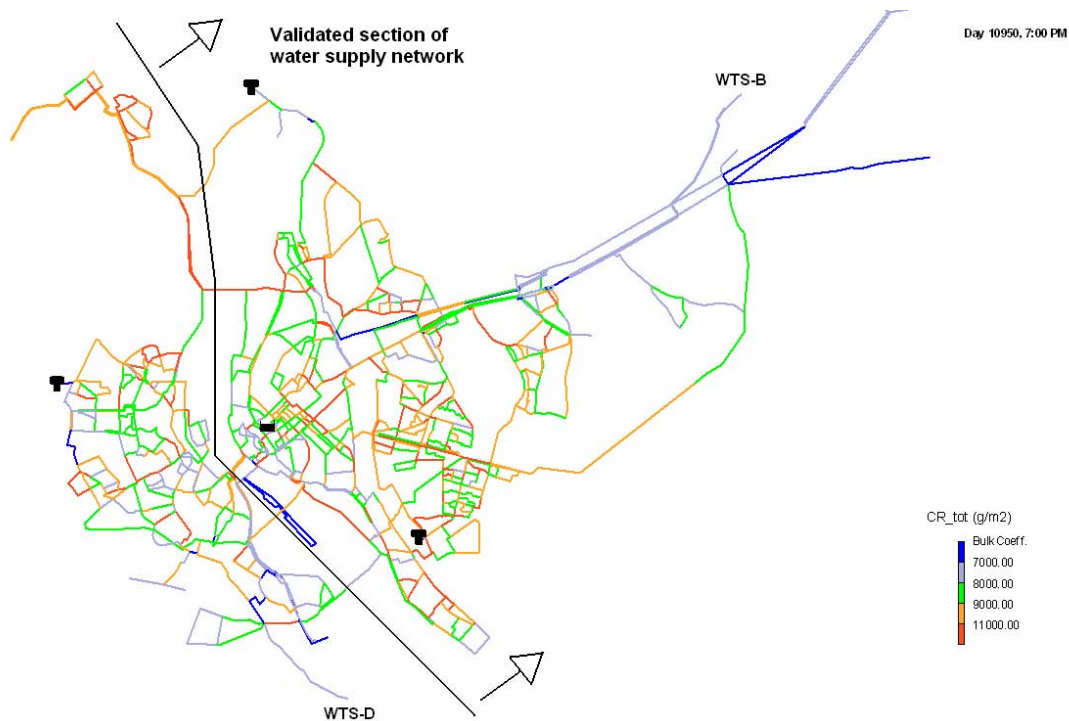


**Fig. B3.** Total corroded mass after 30th year ( $\text{g m}^{-2}$ ).

Title Page

Abstract

Introduction

Conclusions

References

Tables

Figures



Back

Close

Full Screen / Esc

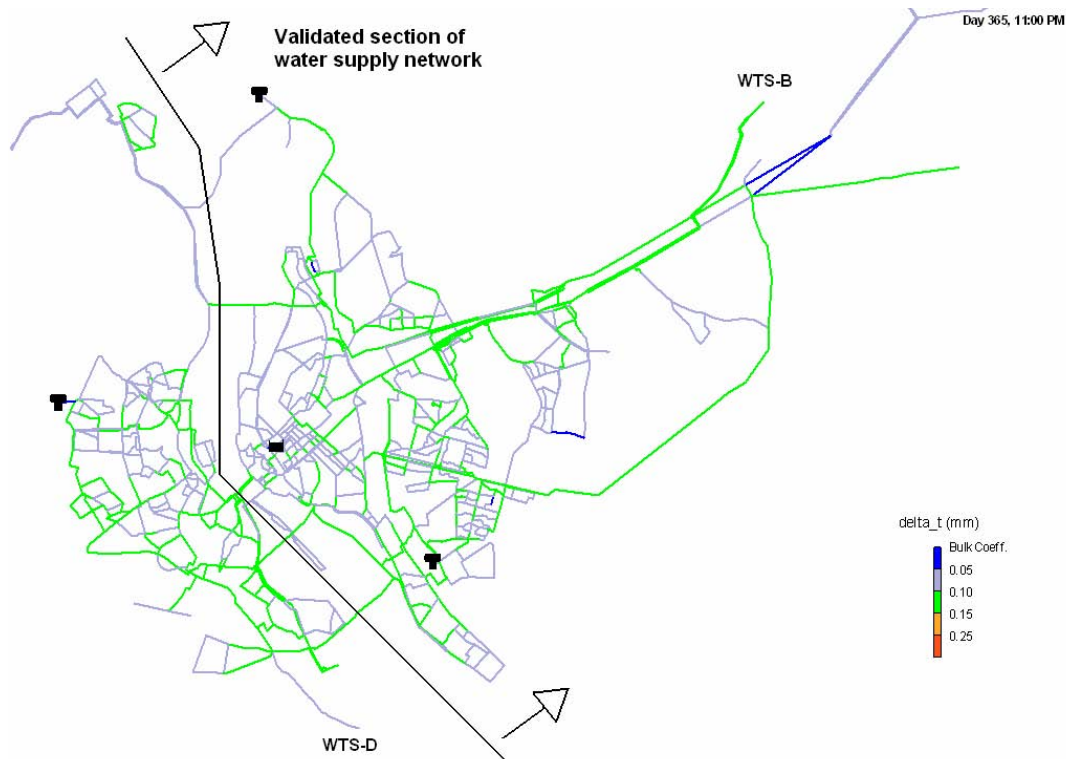
Printer-friendly Version

Interactive Discussion



**Development of a  
iron pipe corrosion  
simulation model**

M. Bernats et al.

**Fig. C1.** Corrosion depth of pipe walls after 1st year (mm).

Title Page

Abstract

Introduction

Conclusions

References

Tables

Figures



Back

Close

Full Screen / Esc

Printer-friendly Version

Interactive Discussion



**Development of a  
iron pipe corrosion  
simulation model**

M. Bernats et al.

Title Page

Abstract

Introduction

Conclusions

References

Tables

Figures



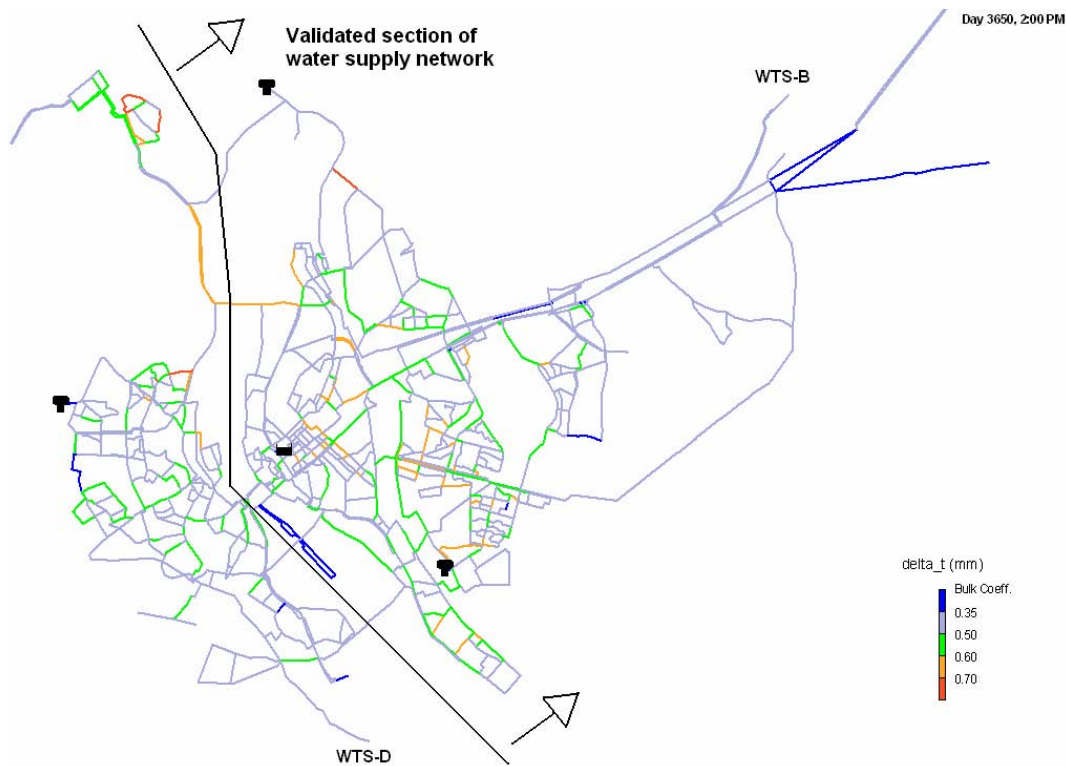
Back

Close

Full Screen / Esc

Printer-friendly Version

Interactive Discussion

**Fig. C2.** Corrosion depth of pipe walls after 10th year (mm).

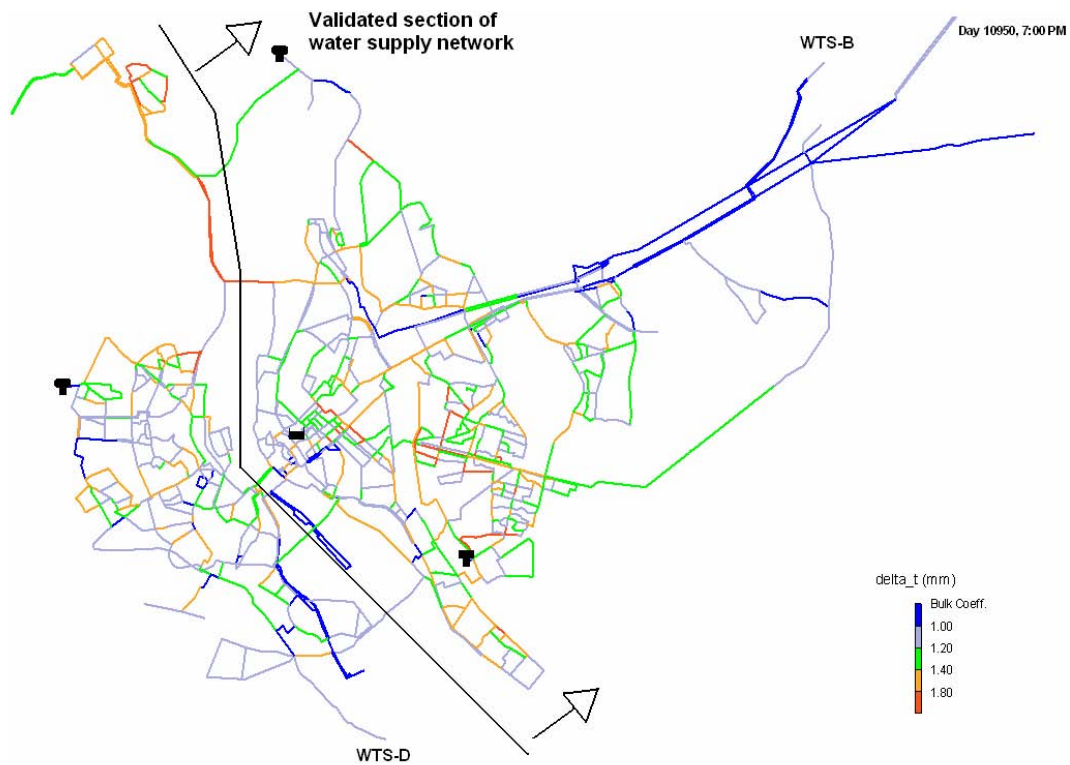


**Fig. C3.** Corrosion depth of pipe walls after 30th year (mm).

## Development of a iron pipe corrosion simulation model

M. Bernats et al.

Title Page

Abstract

Introduction

Conclusions

References

Tables

Figures



Back

Close

Full Screen / Esc

Printer-friendly Version

Interactive Discussion

